An Analogous Model for Modelling Band Structures using Symmetry-Broken Sound Waves

Grant Saggars*
University of Kansas
(Dated: May 5, 2025)

Band structure theory forms the cornerstone of condensed matter physics and underpins the design and functionality of all modern electronic devices. However, developing robust experimental intuition for this quantum mechanical phenomenon remains challenging for students, as direct visualization typically requires sophisticated techniques like angle-resolved photoemission spectroscopy that are financially prohibitive for educational settings. While existing pedagogical approaches using coupled mechanical oscillators provide some insight, they introduce unnecessary layers of abstraction between the model and the quantum reality they represent [1]. We address this pedagogical gap by demonstrating an acoustic wave analogue that directly models electron behavior in periodic potentials. Our approach requires only basic laboratory equipment to create a one-dimensional acoustic lattice that exhibits band formation, allowing students to directly observe, measure, and hear the quantum mechanical principles underlying band structure formation. This accessible experimental platform transforms an abstract quantum concept into a tangible, macroscopic phenomenon that students can explore firsthand, significantly enhancing conceptual understanding of this fundamental solid-state physics principle.

I. INTRODUCTION

The goal of this work is to model a wave (in this case, sound) completely confined to a chain of regions it may occupy. These regions are formed from several lengths of tubing, separated by irises with circular slits in the center. This is analogous to the 1-D tight binding model, an introductory model to discuss electron transport in crystalline materials [2].

Before considering the model of electrons confined to this chain of atoms, it is helpful to imagine the case where it is free to move along the length of the tube. As the frequency, analogous to electron energy, is varied, we expect to observe resonant states at certain ratios to the tube length, L:

$$f_n = n\frac{c}{2L} \tag{1}$$

Where c is the speed of sound, n is a positive integer $n = 1, 2, 3, \ldots \infty$. When we introduce irises, analogous to barriers between atoms, electrons develop overlapping wave functions, violating the orthogonality condition, also called the Bragg condition [3]. This necessitates the formation of bands, when

$$n\lambda = 2a \tag{2}$$

where a is the distance of the reflecting planes. Let the electron wave function in an isolated atom centered at position $\mathbf{R}_n$ be $\phi(\mathbf{r}-\mathbf{R}_n)$. When atoms form a crystal, the total wave function must be a Bloch function:

$$\psi_{\mathbf{k}}(\mathbf{r}) = \sum_n e^{i\mathbf{k}\cdot\mathbf{R}_n}\phi(\mathbf{r}-\mathbf{R}_n) \tag{3}$$

II. ACOUSTIC ANALOGY

Sound waves show a linear dispersion with a slope proportional to sound velocity.

$$f(k) = \frac{c}{2\pi}k \tag{4}$$

Electrons, however, have a parabolic dispersion.

$$E(k) = \frac{\hbar^2}{2m}k^2 \tag{5}$$

This work does not delve deeply into scattering, however, modifications of this so called free-electrion like dispersion are observed when electrons have a wavelength that is comparable to twice the lattice constant, a of the solid. In this case, the electrons are scattered effectively by the periodic lattice.

In the acoustic analog, we introduce periodic scattering centers separated by a distance, a, that is comparable to half the wavelength of sound [4].

The acoustic system consists of a sequence of cylindrical cavities connected by apertures. This creates a periodic modulation of the acoustic impedance analogous to a periodic potential in the electronic case.

III. CONSTRUCTION OF WAVE VECTOR

We identify each resonant peak within a band, $\omega_1, \omega_2, \ldots, \omega_N$, and in ascending order, assign wave vectors according to

$$k_n = \frac{n\pi}{a}, \quad n = 1, 2, \ldots, N$$

* Grant-S@ku.edu

The wavefunction, written in the form of Equation 3, cannot be assigned to a single point in reciprocal space. Instead, it is a sum with contributions from a single k-point in each Brillouin zone. As a result, the dispersion, $E(k)$ is usually plotted only in the first Brillouin zone. This is called the "reduced zone scheme" in contrast to the "extended zone scheme".

IV. EQUIPMENT CONFIGURATION AND FOURIER ANALYSIS

A. Experimental Setup

In this experiment, instrumentation is provided by TeachSpin, however all that is required is a sufficient way to control the speaker output and a way to monitor input from the microphone. There are several analog systems in the equipment used, however this experiment would be made much simpler and more accurate using digital controls. See Figure 1 for the connections and Figure 2 for an example configuration of apertures and tubes. In this work, we use 8x 75mm tubes and 7x apertures with a diameter of 16mm.

A noise-free room is advised to reduce acoustic noise. The nature of this experiment is educational, so this may be taken to whatever extreme available. In our work, we close doors between rooms, lay acoustic dampening foam beside cracks, and collect data when nobody is present. Do note, the microphone itself is only so sensitive, and in many cases acoustic noise is a mild source of uncertainty. Low frequency signals tend to penetrate better than high frequencies, so this experiment will best be done with fewer people in the room to avoid sounds of closing doors, moving chairs, or talking.

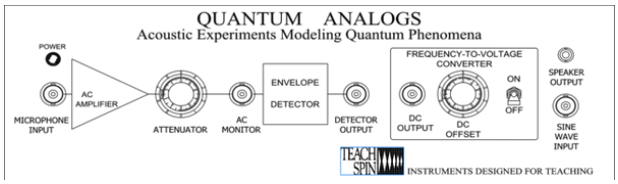

FIG. 1: Schematic of the instrumentation. SINE WAVE INPUT is connected to a signal generator, set to sweep frequency, and output from SPEAKER OUTPUT is passed to the speaker, at one end of the tube. MICROPHONE INPUT is connected to the microphone, located at the other end of the tube. The signal goes through an amplification stage, and output is taken from DC OUTPUT. DC OFFSET is tuned to get a non-clipped signal to display on the oscilloscope in X-Y mode.

Our signal generator is set to sweep the maximum frequency range allowable by the speaker, in this case 100-10k Hz, at at a fixed voltage. The microphone goes through an AC-DC conversion process, where the amplitude of the signal corresponds to frequency. Using this, we are able to preform simple Fourier analysis by collecting a complete spectra from the constructive and destructive interference of the standing wave. It is worth noting that the first peaks in the spectrum are the resonances of the speaker and microphone, and not the sound wave.

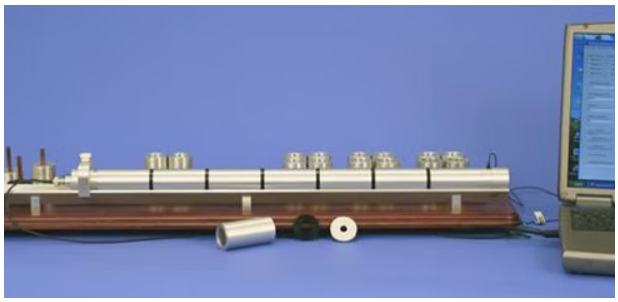

FIG. 2: An example configuration of tubes and apertures, courtesy of TeachSpin.

B. Analysis

Here, our equipment is largely analog, and extremely limited in resolution. In particular, our oscilloscope has 256 points alone that can be collected in the x-y channels. Furthermore, we are unable to directly export data in this format, nor with swept data. To combat the latter, we export an image of the scope trace in image format, and process it as a bitmap. Specifically, at each x-value, we average the pixels y-direction, giving a trace in digital data format.

Our signal resolution is very limited due to the 256x256 pixel screen size, so we take take several scans, first over the whole spectra, then zoomed in on the peaks. We map the low resolution, full sweep from relative to absolute units on the x-axis by means of a simple linear transformation. The high resolution scans are then matched to their location on full sweep scan using another linear transformation with parameters determined by fitting, results of which are described in appendix B.

Peaks still suffer from smearing, and accurately identifying their center is not well done by fitting techniques, as many peaks are ill defined from their neighbors. Instead we take the approach of directly computing the derivative, and selecting points between positive-negative concavity changes, due to the smearing giving ill-defined transitions between maxima. Discrete, measured data is always susceptible to noise, and traditional finite differences calculations will give results with dramatically larger noise. Instead, we apply a noise-resistant technique called Total Variation Regularized Numerical Differentiation [5].

V. DISCUSSION

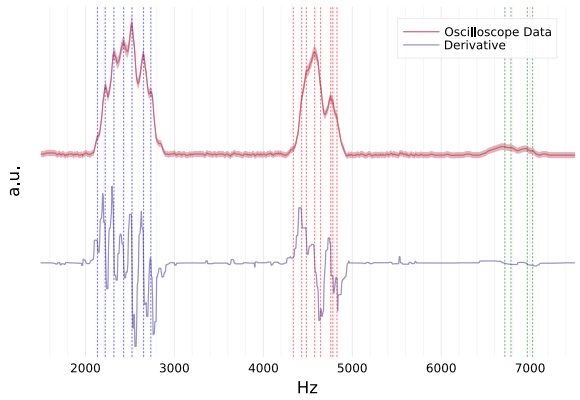

FIG. 3: Fourier analysis where the derivative of our spectrum used to compute peak centers. Three clusters of peaks with diminishing intensity can be seen.

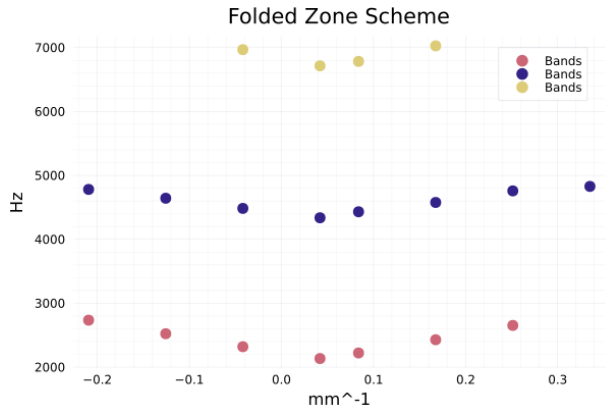

FIG. 4: Band structure of our acoustic analogue system plotted in the reduced zone scheme. The data points represent measured resonance frequencies (ω) versus wave vectors (k) constructed from our experimental setup of eight 75mm tubes separated by seven 16mm apertures. Three distinct energy bands are visible, with band gaps occurring at $k = n\pi/a$ ($n = 1, 2$), demonstrating the formation of forbidden frequency regions analogous to electronic band gaps in crystalline solids.

In this paper, we have demonstrated an acoustic analogue for the quantum mechanical tight binding model, providing a tangible and accessible way to visualize band structures that are fundamental to condensed matter physics. By creating a periodic arrangement of cylindrical cavities connected by apertures, we successfully modeled the essential physics of electron waves in crystalline solids using sound waves.

Our key limitations in this experiment are equipment quality. Use of digital equipment and a computer driven control ought to allow students to accurately observe higher order states and construct a larger band structure. Future improvements should focus on implementing digital data acquisition using computer-controlled frequency sweeping and digital signal processing. This would allow for:

1. Higher frequency resolution to better resolve closely spaced peaks

2. Extended range measurements to observe higher-order bands

3. Automated peak identification to reduce measurement uncertainty

4. Real-time visualization of the developing band structure during measurements

Appendix A: Discussion of Precision and Uncertainty

Throughout this work, we use linear propagation theory for the propagation of all errors via the excellent measurements library in Julia [6].

Our oscilloscope has an uncertainty of 3% + 2 LSD, which is propagated throughout our measurements. There is also some uncertainty associated with fitting high resolution data to the low resolution initial scan, discussed in Figure 5. We obtain large reduced chi-squared values, discussed in Figure 5. Ordinarily this would suggest a statistical discrepancy, however, in fitting high resolution data to low resolution data, do not consider side effects of display settings, where the oscilloscope display does not directly match data collected. Instead, there is some level of anti-aliasing and widening to make the trace human-readable which broadens the trace, obfuscating the valleys and peaks of the data when we take the mean in the y-direction to obtain a curve.We inherently understand that we are measuring the same underlying population, and therefore argue that statistical uncertainty here may be disregarded to a certain degree.

Appendix B: Data Processing Techniques

We fit to the baseline higher resolution spectra using a linear model, shown in Figure 5.

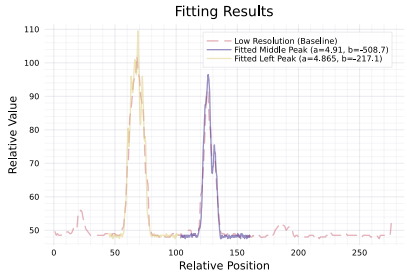

FIG. 5: Higher resolution scans, fitted to the baseline spectrum using a linear model. In this work, we neglect to fit the rightmost grouping of peaks as it was unclear at the time of data collection what this object was. In fitting these, we apply a chi-squared statistical model, and find chi-squared values of 4.78σ and 11.1σ, for the left and right respectively.

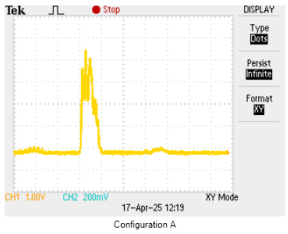

(a) Baseline

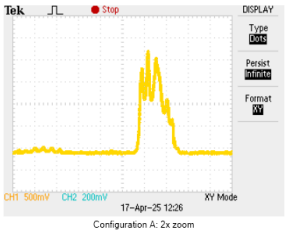

(b) Medium Resolution

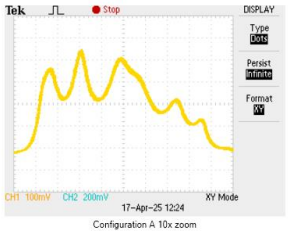

(c) High Resolution

FIG. 6: Sample data collected on the oscilloscope screen of a configuration of 8x irises and tubes. The trace is isolated by masking only the square containing the curve, the value channel extracted, rounding applied to convert the image to a matrix of binary values, then sliced horizontally to find the center of the curve.

[1] I. Neder *et al.*, Bloch oscillations, landau–zener transition, and topological phase evolution in an array of coupled pendula, Proceedings of the National Academy of Sciences 10.1073/pnas.2310715121 (2024).

[2] S. H. Simon, *The Oxford Solid State Basics* (Oxford University Press, Oxford, UK, 2013).

[3] D. Tong, Solid state physics, `https://www.damtp.cam.ac.uk/user/tong/solidstate.html` (2017), lecture notes, University of Cambridge. Permission granted to copy and distribute freely with attribution.

[4] I. TeachSpin and R. Matzdorf, Quantum analogs: Acoustic experiments modeling quantum phenomena, `https://www.teachspin.com/quantum-analogs` (2009), educational apparatus developed in collaboration with Prof. Rene Matzdorf, University of Kassel.

[5] R. Chartrand, Numerical differentiation of noisy, nonsmooth data, International Scholarly Research Notices **2011**, 164564 (2011), https://onlinelibrary.wiley.com/doi/pdf/10.5402/2011/164564.

[6] M. Giordano, Uncertainty propagation with functionally correlated quantities, ArXiv e-prints (2016), arXiv:1610.08716 [physics.data-an].